Build Simul (2021) 14: 1685–1695
https://doi.org/10.1007/s12273-021-0778-7

Multi-objective optimization of thermochromic glazing based on daylight and energy performance evaluation

Xiaoqiang Hong[1] (✉), Feng Shi[1], Shaosen Wang[1], Xuan Yang[1], Yue Yang[2] (✉)

1. School of Architecture and Civil Engineering, Xiamen University, Xiamen, 361005, China
2. School of Mechanical Engineering and Automation, Harbin Institute of Technology, Shenzhen, 518055, China

Abstract

Many efforts have been detected to investigate thermochromic (TC) glazing for improving building energy saving, while only a few approaches for daylight performance analysis. In this study, the performance of TC glazing is investigated based on multi-objective optimization for minimizing energy demand while maximizing daylight availability. The effects of five parameters including transition temperature, solar transmittance in clear state, solar transmittance modulation ability, luminous transmittance in clear state, and luminous modulation ability on the building energy consumption and useful daylighting illuminance ($UDI_{300-3000}$) are examined. Linear Programming Technique for Multi-dimensional Analysis of Preference (LINMAP) is used for the decision-making of Pareto frontier. This research aims to explore the ideal thermochromic glazing by considering the daylight and energy performance of a typical office room, taking the weather condition of Xiamen, China as an example. Although it is impossible to achieve both optimal values of energy consumption and $UDI_{300-3000}$ simultaneously, the proposed multi-objective optimization method could still provide low energy consumption with sufficient daylight. The non-dominated sorting of Pareto optimal solution (POS) demonstrated that the optimum building energy consumption and $UDI_{300-3000}$ for single glazed windows are 46.64 kWh/m^2 and 70.92%, respectively, while the values for double glazed windows are 44.40 kWh/m^2 and 71.88%, respectively. The selected hypothetical TC windows can improve the building energy and daylighting performance simultaneously when compared with traditional clear single and double glazed windows. The presented framework provides a multi-objective optimization method to determine the most suitable TC glazing technologies for designers and architects during the design and retrofit procedure.

Keywords

thermochromic;
transition temperature;
daylighting;
building energy performance;
multi-objective optimization

Article History

Received: 01 November 2020
Revised: 06 January 2021
Accepted: 02 February 2021

1 Introduction

Solar radiation transmitted through the transparent envelope is a decisive contributor to the daylight availability (Baetens et al. 2010) and the heat gain into buildings (Zheng et al. 2019), which accounts for the dominant factor of cooling loads. With the appropriate passive design of the transparent envelope, a building has the potential to make full use of solar radiation to deliver combined improvements in building energy and daylight performance. Many innovative technologies have been developed to fulfill the radiation control function for the transparent envelope, including reflective film (Chen et al. 2015; Soumya et al. 2015), low-E (Guo et al. 2011), thermochromic (TC) (Tällberg et al. 2019), photochromic (Ataalla et al. 2018), electrochromic (Garcia et al. 2013), gasochromic (Feng et al. 2016), transparent insulation materials (Sun et al. 2018) and dynamic shadings (Hosseini et al. 2019).

Among them, vanadium dioxide (VO_2) based TC glazing can adjust its optical properties at a switching (or transition) temperature (τ_t) reversibly (Aburas et al. 2019), and thus varying its throughput of the solar radiation responding to the environmental conditions in a dynamic way: blocking the undesired solar heat gain at high temperature while achieving high transmittance at low temperature. Many efforts have been taken to enhance the TC performance

E-mail: hongxq@xmu.edu.cn (Xiaoqiang Hong); yangyue2017@hit.edu.cn (Yue Yang)

List of symbols

A	area (m²)
COP	coefficient of performance (—)
E	electricity power (kWh)
EPA	electric power consumption per unit indoor area (kWh/m²)
$F(X)$	vector of objective function (—)
g	inequality constraints
G	solar irradiation (W)
h	equality constraints
p	number of inequality constraints
q	number of equality constraints
Q	energy consumption (kWh)
T	transmittance
X	vector of decision variables (—)
TC	thermochromic (—)
τ	temperature (°C)

Subscripts

c	cooling
c&h	cooling and heating
h	heating
lighting	artificial lighting
lum	luminous
k	decision variables
solar	solar

(Blackman et al. 2009; Huang et al. 2013; Li et al. 2014; Cao et al. 2020): reducing the τ_t to room temperature, enhancing the luminous transmittance and solar energy modulation, thus making it next-generation energy-efficiency building material for opaque (Fabiani et al. 2019; Hu and Yu 2019a,b; Zhang and Zhai 2019; Fabiani et al. 2020; Zhang et al. 2020) and transparent envelope (Aburas et al. 2019) application. Zhang et al. (2019) designed and fabricated a perovskite TC smart window which could achieve a high solar modulation ability of 25.5%. Some other recently developed thermochromic coatings for smart windows have been summarised in Cui et al. (2018).

Many studies have been conducted to investigate the energy-saving performance of the TC glazing window experimentally and theoretically (Long and Ye 2016). Lee et.al conducted field test measurements to demonstrate the energy-efficiency performance of the buildings with TC windows in Denver (Lee et al. 2013a) and California (Lee et al. 2013b) (USA). And they found that the ideal critical switching temperature for TC glazings should be determined based on zone heat balance rather than ambient air temperature (Lee et al. 2013b). Ye et al. (2013) conducted outdoor tests to investigate building energy performance of the TC single glazing, double glazing (Long et al. 2015), and the synergetic application of TC glazing and phase change material (Long et al. 2014) in Hefei (China). They found that the test room with the TC glazing could save up to 21.7% (Long and Ye 2017) cumulative cooling load than that with ordinary clear glazing using the indexes of energy saving equivalent (ESE) and energy saving index (ESI) (Ye et al. 2014). Saeli et al. (2010a,b) performed the energy modeling studies to assess the energy-saving performance of TC glazing compared with Low-E and tinted absorbing glazing used in double-glazed window and found that the energy savings was significant for warmer climates. The simulation works done by Hoffmann et al. (2014) also showed the energy saving and visual comfort benefits of a series of double-glazed TC windows with different transition temperatures in hot climates. Warwick et al. (2014) investigated the effect of TC transition gradient and found that the TC glazing with a sharp hysteresis gradient could reduce 51% energy demand compared to a standard double glazed system. Liang et al. (2018, 2019) analyzed the building energy performance, daylight and visual comfort of different types of TC glazing applied in the double-glazed window under five climatic conditions in China. Giovannini et al. (2019) evaluated the energy performance and daylight availability of a ligand exchange thermochromic glazing in an office space.

Most of the existing studies for the building application of TC windows were carried out for the annual energy saving analysis, while far less for visual comfort analysis (Aburas et al. 2019). Besides, only limited types of TC film were analyzed from a building performance perspective. The ideal properties (i.e. transition temperature τ_t, solar transmittance in clear state T_{solar}, solar energy modulation ΔT_{solar}, luminous transmittance in clear state T_{lum}, and luminous modulation ΔT_{lum}) of TC materials considering building energy-efficiency and daylight performance simultaneously remain unclear. This research aims to explore the multi-objective optimized performance of single and double glazed windows applied with TC materials, which targets the minimization of energy usage and the optimization of daylight availability. The impacts of the properties of TC materials on the building energy consumption and desired annual daylight hours within the useful daylight illuminance ($UDI_{300-3000}$) will be analyzed, and the multi-objective trade-off optimization will be conducted via multi-objective particle

swarm optimization (MOPSO) approach to find out Pareto frontier for single and double glazed windows. Finally, the optimal properties of TC glazing obtained from the Pareto optimal solution (POS) will be determined.

2 Methodology

2.1 Building performance simulation

In this research, Rhinoceros 3D graphics software and Grasshopper plugin are used to generate parametric models (Eltaweel and Su 2017). Grasshopper plugins, namely Ladybug and honeybee (Mostapha and Sarith 2016), were used as engines for EnergyPlus, which was a widely accepted building simulation program for the studies of TC windows and other advanced glazing systems (Saeli et al. 2010a; Hoffmann et al. 2014; Warwick et al. 2014; Liang et al. 2018), to get the building energy and daylight performance analysis. The location of Xiamen (24.27°N latitude, 118.06°E longitude), in hot summer and warm winter zone, one of the five major climatic zones of China, was selected. Xiamen has a low latitude, which resulted in significantly different solar altitudes and solar intensity on the south-facing façade during summer and winter. By running the annual simulations in Xiamen, the various environmental impacts on the daylight and energy performance of TC glazing could be largely explored. The Chinese Standard Weather Data (CSWD) of Xiamen can be downloaded from (Weather Data from EnergyPlus) by using the Ladybug plugin.

As shown in Figure 1, a single-zone office room with dimensions of 4.0 m × 4.0 m × 4.0 m (length × depth × height) was chosen for the simulation. The external wall was constructed with concrete blocks covered with cement plaster on both sides, and the specifications are shown in Table 1. Only the south envelope placed with a window was exposed to outdoor conditions, while the other walls were considered as adiabatic and expected to yield no heat transfer, standing for a south-facing and midfloor office room within a multi-story building in the northern hemisphere. Assuming a moderate-area window without shading devices, the window-to-exterior-wall-area ratio (WWR) was fixed as 0.4. In subtropical Xiamen, single glazed fenestration and double glazed fenestration dominate the façades of many pre-green buildings and new buildings, respectively. Thus, both single glazed windows and air-filled double glazed windows were individually simulated in this study. Table 2 shows the properties of clear glazing. TC film was coated on the external glazing of the double glazed window. A TC film with excellent ΔT_{solar} of 36%, high T_{lum} of 56%, and τ_t of 50 °C was selected (Yang et al. 2017). Five illuminance sensors were designated at the working plane with a distance of 0.8 m from the floor: one sensor is in the center of the room and the other four sensors are uniformly distributed on the plane.

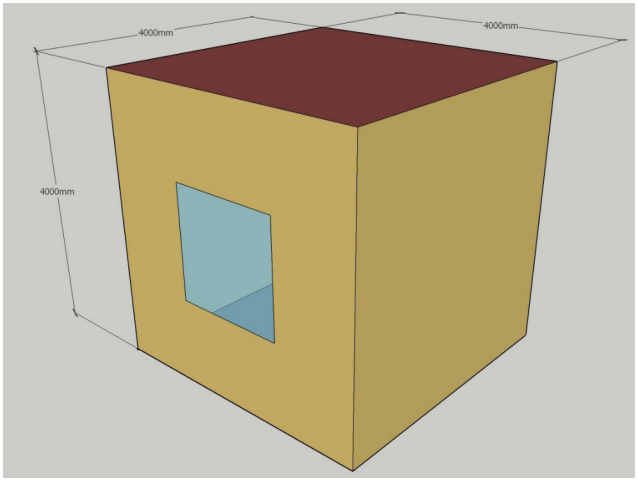

Fig. 1 Schematic of the sample office room for BES in EnergyPlus

Table 1 Specifications of the wall construction

Parameters	Unit	20 mm cement plaster	200 mm low-density concrete block
Roughness	—	Smooth	Medium rough
Thickness	m	0.02	0.2
Thermal conductivity	W/(m·K)	0.727	0.571
Density	kg/m^3	1602	609
Specific heat	J/(kg·K)	840	840
Thermal absorptance	—	0.9	0.9
Solar absorptance	—	0.4	0.5
Visible absorptance	—	0.4	0.5

Table 2 Glazing material properties

Parameters	Single glazing (where TC coated)	Double glazing 1.3 cm air	
		Ouside (where TC coated)	Inside
Thickness (mm)	6	6	6
Conductivity(W/(m·K))	1.4	1.4	1.4
Solar transmittance	0.78	0.78	0.78
Solar reflectance	0.08	0.08	0.08
Visible transmittance	0.88	0.88	0.88
Visible reflectance	0.06	0.06	0.06
Infrare transmittance	0.00	0.00	0.00
Infrared hemispherical emissivity	0.84	0.84	0.84

The design internal loads of the building zone and the daily operating schedules were summarized in Table 3 and Figure 2, respectively, according to the building energy efficiency standards in China (JGJ/T449 2018). The schedules of the indoor heating and cooling set-point were shown in Figure 3. The artificial lights were controlled by a

Table 3 Design loads of the building zone

Load	Unit	Intensity
Occupancy	m^2/person	8
Lighting	W/m^2	15
Heat gain from equipment	W/m^2	15
Heat gain from occupants	W/person	134
Fresh air	m^3/(h·person)	30

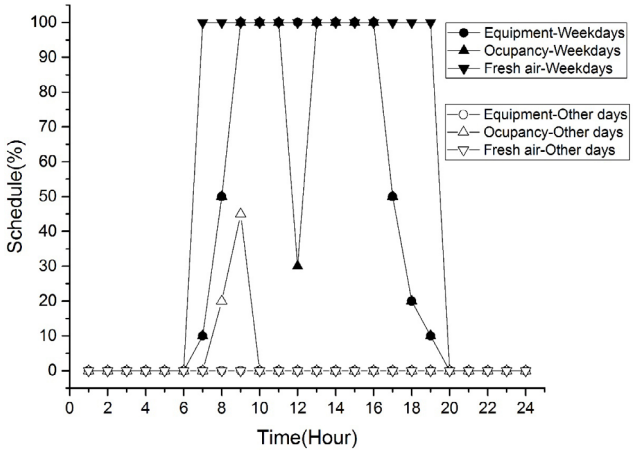

Fig. 2 Operating schedules of various loads

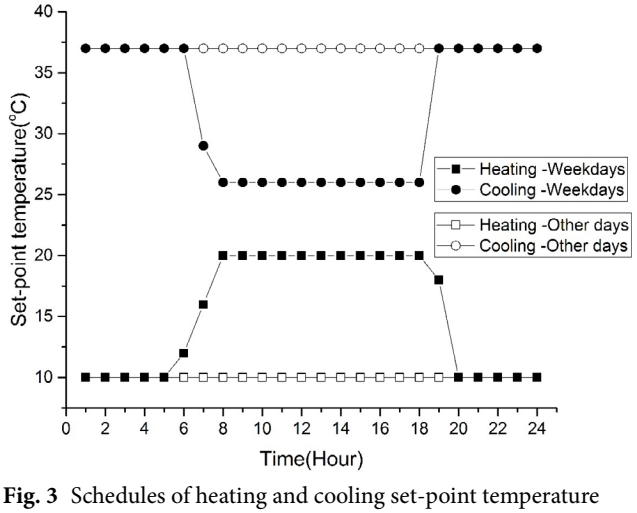

Fig. 3 Schedules of heating and cooling set-point temperature

continuous/off lighting control system in EnergyPlus, to meet the desired illuminance level of 500 lux at the working plane during the occupancy hours (BSI 2011). In EnergyPlus, the zone heat balance calculations include surface and air components. TRAP and DOE-2 algorithms (DOE 2016) were selected for the simulations of the inside and outside surface convection, respectively. And the heat conduction through the walls was calculated using Conduction Transfer Function (CTF) solution algorithm. Ideal air load was used to estimate the annual cooling and heating energy consumption of the office room.

The electric power consumption for cooling and heating is calculated by:

$$E_{c\&h}=Q_c/\mathrm{COP}_c+Q_h/\mathrm{COP}_h \quad (1)$$

where Q_c and Q_h are the cooling energy consumption and the heating energy consumption, respectively; COP_c and COP_h are the coefficients of performance of standard cooling facility and heating facility, respectively. In this paper, COP_c and COP_h were set to the recommended 2.5 and 2.2, respectively (JGJ/T449 2018).

The total electric power consumption per unit indoor area is defined as:

$$\mathrm{EPA}=\left(E_{\mathrm{lighting}}+E_{c\&h}\right)/A_{\mathrm{indoor}} \quad (2)$$

where E_{lighting} is the electric power for artificial lighting, and A_{indoor} is the indoor area of the sample office room.

The useful daylighting illuminance (UDI) metric is calculated to assess the percentage of occupied hours in which the indoor horizontal daylight illuminance of a specific point falls within a specific illuminance range (Liang et al. 2018) for the illuminance sensors. This metric can describe the spatial mean illuminance value (Abdollahzadeh et al. 2020). Three illumination evaluation levels for the indoor area, namely "daylit", "partially daylit" and "overlit" areas, were used as suggested in other studies (Mahmoud and Elghazi 2016). The area with illuminance lower than 300 lux ($\mathrm{UDI}_{<300\mathrm{lux}}$) was defined as a "partially lit" area; The area with illuminance greater than 3000 lux ($\mathrm{UDI}_{>3000\mathrm{lux}}$) was defined as "overlit"; The area archives illuminance levels between 300 lux and 3000 lux ($\mathrm{UDI}_{300-3000}$) was defined as "daylit". In this way, the UDI within the range of 300–3000 lux was supposed to be useful and satisfied with the designed illuminance.

2.2 Multi-objective optimization

Multi-objective optimization has been widely applied in multiple criteria decision making for satisfying several objectives simultaneously. As the objectives are often two or more conflicting outcomes, the optimal decisions can be made by multi-objective optimization to quantify the trade-offs between these objectives and figuring out the best solution for decision-makers.

A multi-objective optimization problem can be expressed as:

$$\min(\max)F(X)=\left[f_1(X),f_2(X),f_3(X),\ldots,f_n(X)\right]^{\mathrm{T}} \quad (3)$$

which is subject to constraint equations as follows:

$$g_i(X)\le 0,\quad i=1,\ldots,p$$

$$h_j(X)=0,\quad j=1,\ldots,q$$

$$x_{k,\min} \le x_k \le x_{k,\max}$$

where X denotes the vector of decision variables, $F(X)$ represents the vector of the objective function, $g_i(X)$ is the inequality constraints, p is the number of inequality constraints, $h_j(X)$ is the equality constraints, q is the number of equality constraints, $x_{k,\min}$ and $x_{k,\max}$ are the lower and upper bounds of the decision variables, respectively. When p and q are both equal to zero, the problem is an unconstrained optimization problem.

The objectives can be maximum or minimum the objective functions, which can be transferred to each other by:

$$\min\{f(x)\}=\max\{-f(x)\} \tag{4}$$

Five key parameters are chosen as decision variables for TC optimization, including transition temperature τ_t, solar transmittance at low-temperature T_{solar}, solar transmittance modulation ΔT_{solar}, luminous transmittance at low-temperature T_{lum}, and luminous modulation ΔT_{lum}. The vector of decision variables is expressed as follows:

$$X = [\tau_t, T_{solar}, \Delta T_{solar}, T_{lum}, \Delta T_{lum}]^T \tag{5}$$

As about half of the solar energy over the full solar spectrum (300–2500 nm) is emitted in the visible spectrum (380–780 nm) (Hoffmann et al. 2014), there is a limitation among the luminous transmittance, solar transmittance and the transmittance in the other spectral regions (300–380 nm & 780–2500 nm). Assuming that the value of the solar transmittance is the arithmetical average of the luminous transmittance and transmittance in the other spectral regions, the following assumptions and constraints should be satisfied.

$$0 \le \Delta T_{solar} \le T_{solar}, \quad 0 \le \Delta T_{lum} \le T_{lum}, \quad 0 \le 2T_{solar} - T_{lum} \le 100\%,$$
$$0 \le 2(T_{solar} - \Delta T_{solar}) - (T_{lum} - \Delta T_{lum}) \le 100\% \tag{6}$$

Regarding the daylight and energy performance, the total electric power consumption (Eq. (2)) and the UDI within the range of 300–3000 lux ($UDI_{300-3000}$) are selected as the objective functions. The present study is focused on minimizing the energy consumption, including cooling, heating and artificial lighting consumptions, while maximizing the desired annual daylight hours, by maximizing the value of $UDI_{300-3000}$.

Among various multi-objective optimization techniques, the hypervolume-based evolutionary optimization (HypE) algorithm is an effective algorithm (Bader and Zitzler 2011) based on Monte Carlo simulation (Bader et al. 2010). Octopus, which is a plugin of Grasshopper, is used to conduct the multi-objective optimization (Pilechiha et al. 2020). The reference point is crucial to the hypervolume indicator of a point set. The HypE algorithm developed in Octopus repeatedly modifies the reference point based on the objective values at each step. As the objectives of the multi-objective optimization problems are often in conflict, i.e. one objective improves while another deteriorates, the outcome is a set of optimal Pareto solutions, which are non-dominated for there are no other solutions to improve all the objectives simultaneously. After the Pareto solutions are identified, decision-makers can choose from these solutions based on the interests of different possible stakeholders. Figure 4 shows the workflow of the optimization progress consists of the inputs, the outputs, the connections, and the optimization algorithm.

The Linear Programming Techniques for Multi-dimensional Analysis of Preference (LINMAP) is a suitable decision-making method for Pareto frontier. The process of LINMAP is usually performed with the aid of a hypothetical point (ideal point) with the best value of objective functions simultaneously while not existing actually. The point in the Pareto frontier which is nearest to the ideal point based

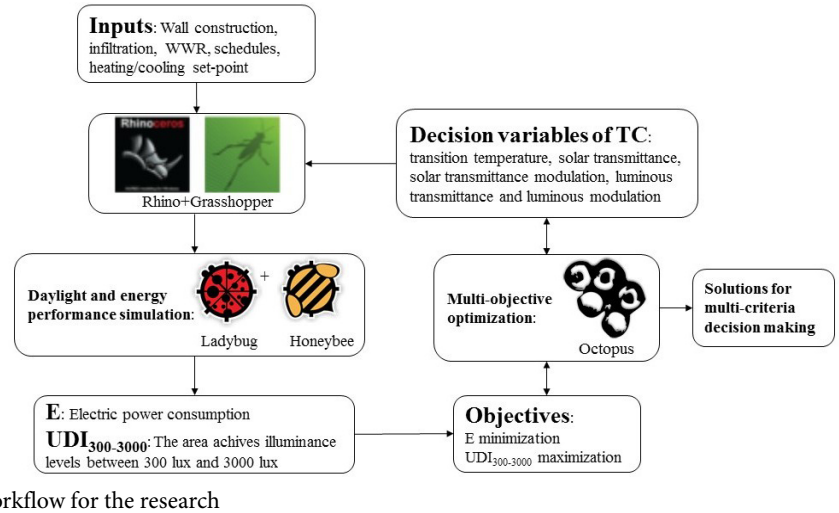

Fig. 4 Scheme of the workflow for the research

on geometric distance after normalization of the objective function values is chosen as the desired solution and defined as the Pareto-optimal solution (POS), as shown in Figure 5.

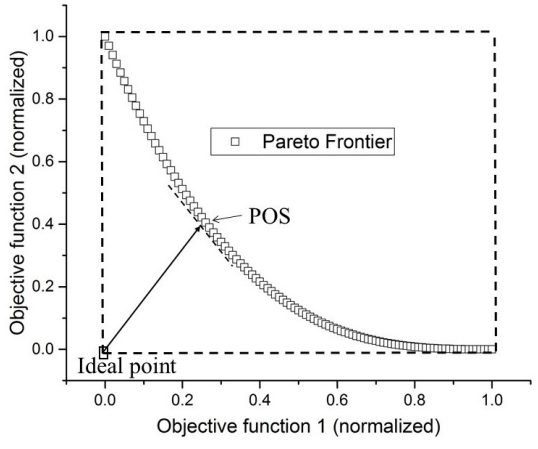

Fig. 5 The schematic diagram of the Pareto frontier

3 Results and discussion

To evaluate the effects of the TC parameters on building energy consumptions and $UDI_{300-3000}$, the first set of the TC is characterized using the parameters reported by Yang et al. (2017), which shows excellent thermochromic performance among the TC glazings in Cui et al. (2018), with transition temperature τ_t of 50 °C, solar transmittance T_{solar} of 36.0%, solar transmittance modulation ΔT_{solar} of 56% and luminous modulation ΔT_{lum} of 7.2%. As the luminous transmittance T_{lum} was not reported in Yang et al. (2017), the values are assumed to be the same as T_{solar}. As the optical properties of most current VO_2 based TC glazing are switched by increasing its solar absorptivity after changing into the metallic state, i.e. reflectance remains constant in metallic and semiconductor state (Ye and Long 2014), the solar reflectance is assumed to be constantly 0.1 in this study. According to the review work on the subjects of thermochromic coatings (Cui et al. 2018; Aburas et al. 2019), the transmittance of the experimental TC for building application varies between 0.288 and 0.78. And the transition temperature varies between 20 °C and 75 °C. In order to study a larger range of the TC coatings, the boundaries of decision variables for multi-objective optimization are extended and shown in Table 4. For reference, the results of the building energy consumption and $UDI_{300-3000}$ for the reference (clear) single and double glazed windows are given in Table 5.

3.1 Effects of decision variables on system performance

The variations of building energy consumption and $UDI_{300-3000}$ with a transition temperature of TC for single and double glazed windows are illustrated in Figure 6. It can be observed that the variations for single and double glazed windows present a similar trend. With the increasing transition temperature, the energy consumption decreases at first and then increases, while $UDI_{300-3000}$ first increases and then decreases. The desired transition temperature of TC glazing varies with the weather conditions, optical properties of TC materials, building types, building orientations, etc. Under the conditions in this study, the TC with the transition temperature of 28 °C achieves the smallest energy consumptions for both single and double glazed windows. And the transition temperatures of 30 °C and 36 °C are more desirable to achieve a better indoor daylight environment for single and double glazed windows, respectively. Thus a transition temperature slightly higher than room temperature is desired for both daylight and energy performance, which is similar to the previous findings that a suitable higher transition temperature for residential applications suggested

Table 4 Decision variables and their lower and upper boundaries

Decision variables	Lower bound	Upper bound
Transition temperature (°C)	10	50
Solar transmittance (—)	0.1	0.9
Solar transmittance modulation (—)	0	0.9
Luminous transmittance (—)	0.1	0.9
Luminous modulation (—)	0	0.9

Table 5 Electric power consumption per unit indoor area and $UDI_{300-3000}$ of the reference single and double glazed windows

	EPA (kWh/m^2)	$UDI_{300-3000}$
Clear single glazed window	46.8	0.639
Clear double glazed window	46.4	0.655

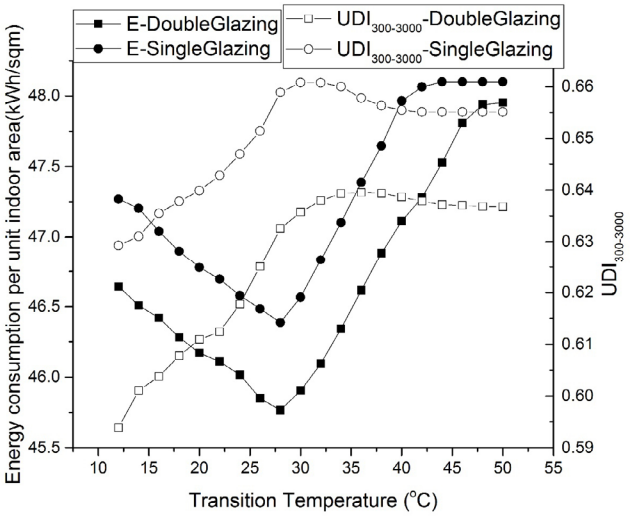

Fig. 6 Variations of building energy consumption and $UDI_{300-3000}$ with transition temperature

by Long et al. (2015), the desired transition temperature at room temperature suggested by Xu et al. (2012) and a low transition temperature (i.e., 20 °C) being not essential suggested by Liang et al. (2018). This is because that the TC glazing with higher transition temperature results in more clear hours and thus more solar irradiance entering the room, while the TC glazing with lower transition temperature results in more tinted hours and thus less solar heat gain. An ideal TC transition temperature is expected to achieve tinted state in the cooling demand period while clear state in the heating demand period, when the amount of daylight within the space is sufficient.

To evaluate the building performance for the optical properties of TC, the transition temperature is characterized using the desired temperature above, i.e. 28 °C. Figures 7 and 8 depict the variation of building energy consumption for the single and double glazed windows with solar transmittance and solar transmittance modulation ability of TC. When the solar transmittance in clear state of TC varies from 0.4 to 0.9, the building energy consumption increases from 45.37 kWh/m^2 to 50.26 kWh/m^2 (10.8%) for the single glazed window, and from 44.56 kWh/m^2 to 49.70 kWh/m^2 (11.5%) for the double glazed window. When the solar transmittance modulation ability varies from 0 to 0.5, the building energy consumption of the single glazed window presents a reduction from 48.47 kWh/m^2 to 45.62 kWh/m^2 (5.9%), while the double glazed window decreases from 48.38 kWh/m^2 to 44.79 kWh/m^2 (7.4%). Some studies found that solar transmittance of TC glazing should be as low as possible in tinted state and vice-versa in clear state (Long and Ye 2014; Ye and Long 2014). However, low solar transmittance in both clear state and tinted state is found to be most suitable for hot climates. The difference between these two studies is that the studied parameters of solar transmittance in tinted/clear state in the previous study, while the parameters of solar transmittance in clear state and solar transmittance modulation ability in the present study. The phenomenon can be explained as the increasing solar transmittance enables more solar irradiance entering the room, resulting in an increase in cooling load and a decrease in heating load. Nevertheless, the cooling energy demand is dominant in subtropical Xiamen. The effect of increasing cooling energy consumption would outweigh that of the decreasing heating energy consumption. As a result, the building energy consumption exhibits an increasing trend with the solar transmittance of TC while a decreasing trend with solar transmittance modulation ability.

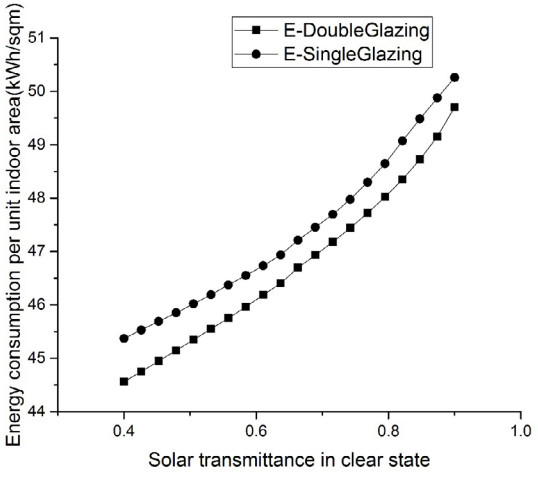

Fig. 7 Variations of building energy consumption with solar transmittance in clear state

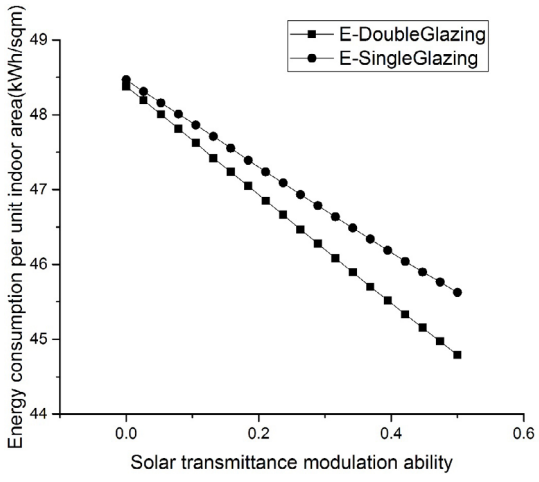

Fig. 8 Variations of building energy consumption with solar transmittance modulation ability

Figures 9 and 10 illustrate the variations of building energy consumption and $UDI_{300-3000}$ with luminous transmittance in clear state and luminous transmittance modulation ability of TC for single and double glazed windows. It can be found that the energy consumption decreases with the increasing luminous transmittance in clear state, while presents a reverse trend with the increasing luminous transmittance modulation ability, i.e. decreasing luminous transmittance in tinted state. With an increasing luminous transmittance in clear state, $UDI_{300-3000}$ tends to firstly increase and then slightly decrease. And with an increasing luminous transmittance modulation ability, $UDI_{300-3000}$ tends to slightly increase first and then decrease. This phenomenon can be explained as followed: the luminous transmittance in tinted state increases with the decreasing luminous transmittance modulation ability. And the increasing luminous transmittance in clear/tinted state enables more daylight transfer into the indoor, resulting in a decrease in energy use for artificial lighting and thus in total building energy consumption. Besides, the increase of luminous transmittance ensures more natural light entering buildings and enhances the indoor illuminance level. And thus, more percentage of working hours within the desired

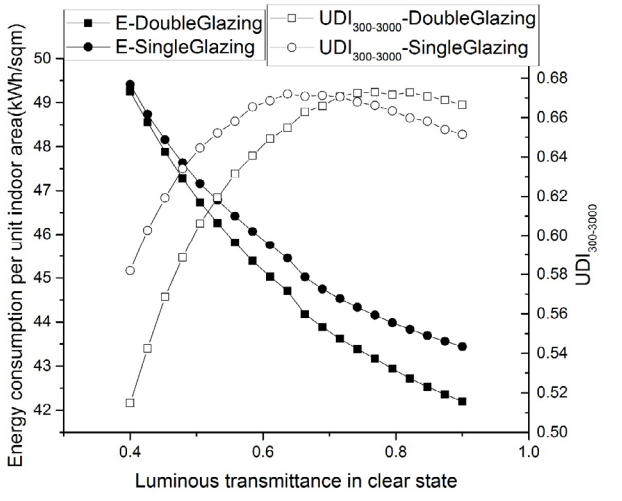

Fig. 9 Variations of building energy consumption and $UDI_{300-3000}$ with luminous transmittance in clear state

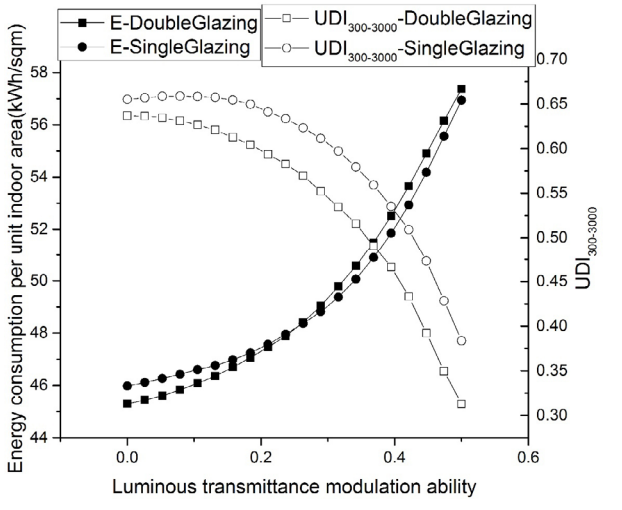

Fig. 10 Variations of building energy consumption and $UDI_{300-3000}$ with luminous transmittance modulation ability

daylighting range ($UDI_{300-3000}$) could be achieved. With the further increase of the luminous transmittance, more accessible daylighting would over-supplying illuminance (over 3000 lux) and increasing the risk of glare. The results indicate that a TC glazing with a higher luminous transmittance glazing is desirable to reduce the building energy use and enhance the indoor daylighting performance, which is consistent with the results by other researchers (Lee et al. 2013b; Liang et al. 2018), and the luminous transmittance modulation ability should not be too high.

3.2 Bi-objective optimization based on Pareto frontier solution

To choose the optimal trade-off solution between minimizing total energy consumption and maximizing daylight comfort, bio-objective optimization is conducted based on the HypE algorithm. The population size is set as 60 and the number of max generation is set as 300. The parameters in Table 4 are selected as the decision variables, which should be subject to constrain conditions.

Figure 11 shows the Pareto frontier solution for the TC coated single and double glazed windows regarding energy consumption and $UDI_{300-3000}$. It can be seen that there is a clear trade-off between building energy performance and daylight performance. With the increasing $UDI_{300-3000}$, the building energy consumption increases moderately at first and then rises rapidly, which means that the cost for improvement of daylight performance will cause deterioration of the energy performance. The best daylight performance is 71.63% in $UDI_{300-3000}$ with the worst energy performance (47.55 kWh/m^2) for the single glazed window, which exists at point B, and 72.07% in $UDI_{300-3000}$ with the worst energy performance (45.45 kWh/m^2) for the double glazed window. Meanwhile, the best energy performance is 46.21 kWh/m^2 with the worst daylight performance (67.65% in $UDI_{300-3000}$) for single glazed window, which exists at point A, and 44.28 kWh/m^2 in best energy performance with worst daylight performance (70.42% in $UDI_{300-3000}$) for the double glazed window.

As there is no point of maximum $UDI_{300-3000}$ and minimum energy consumption simultaneously, the decision-making process is performed using LINMAP to determined the POS. As observed in Figure 11, the POS is the point C with building energy consumption of 46.64 kWh/m^2 and $UDI_{300-3000}$ of 70.92%% for single glazed window, and the point C′ with building energy consumption of 44.40 kWh/m^2 and $UDI_{300-3000}$ of 71.88% for the double glazed window. The optimized TC window led to building energy saving of 0.34% and increase of the desired range illumination $UDI_{300-3000}$ of 10.9% when compared with traditional clear

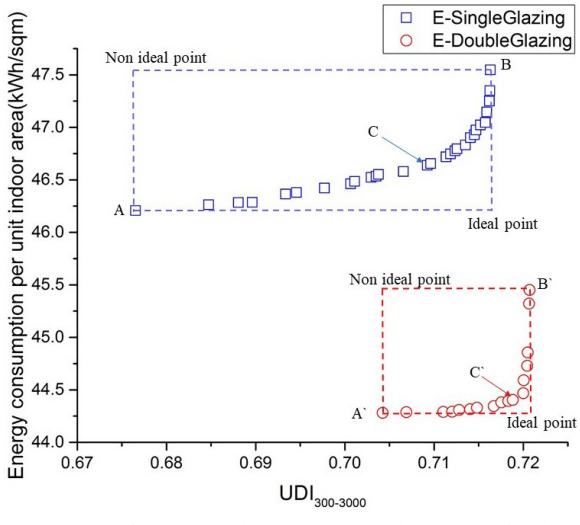

Fig. 11 Pareto frontier and Pareto optimal solution for the TC coated single and double glazed windows

single glazing, and building energy saving of 4.31% and increase of the desired range illumination $UDI_{300-3000}$ of 9.8% when compared with traditional clear double glazing. This indicates that the switching features of TC material could not only reduce building energy consumption by modulating the solar heat gains through windows, but also regulate daylight and reduce visual discomfort caused by excessive daylighting. The detailed optimum designed parameters of points A–C are shown in Table 6. It can be found that the optimum transition temperature tends to be slightly higher than the indoor air temperature, which is in the range of 28.7–34.8 °C for the single glazed window and 29.2–33.3 °C for double glazed windows. The optimum visual transmittance in clear state is located in the range of 0.73–0.76 for single glazed window, while in the upper boundary (0.89 to 0.90) for double glazed windows. The optimum solar transmittance in clear state is the smallest value that subjects to constraint conditions, indicating that the TC windows with higher luminous transmittance and lower solar transmittance are more desired for subtropical climates. This is because a TC window with high visible transmittance allows more accessible daylighting. As there are two panels in a double glazed window that blocking more daylighting, the optimum visible transmittances of TC for double glazed windows are higher than that for single glazed windows. As the solar heat gain is substantial throughout the year for commercial buildings in subtropical Xiamen, TC glazing with lower solar transmittance is more desired to reduce the penetration of solar energy for building energy efficiency. Furthermore, the optimum values of the modulation abilities for solar transmittance and visual transmittance varies. This indicates that the modulation abilities are not the higher the better. The optimum values of the modulation abilities for visual transmittance in all points are higher than the values for solar transmittance because of the lower and upper bounds in the constraints.

4 Conclusion

This study established a multi-objective optimization model using Rhinoceros software to investigate the daylight and energy performance for single and double glazed windows with thermochromic (TC) glazing in a sample office room. Taking the weather condition of Xiamen in China as an example, the optimization objectives were minimizing building energy usage while maximizing received desired daylight. The building energy usage and daylight were calculated using Grasshopper plugins: Ladybug and Honeybee. The effects of five key parameters including transition temperature, solar transmittance in clear state, solar transmittance modulation, luminous transmittance in clear state, and luminous modulation were examined. Meanwhile, the trade-offs between building energy consumption and useful daylighting illuminance metric ($UDI_{300-3000}$) were analyzed by using the HypE optimization algorithm, which is applied using a Grasshopper plugin: Octopus. The following conclusions can be drawn:

(1) A transition temperature slightly higher than room temperature was desired for both daylight and energy performance in Xiamen. The transition temperature of 28 °C achieved the smallest energy consumptions for both single and double glazed windows. And the transition temperatures of 30 °C and 36 °C were desirable to obtain the best indoor daylight performance for single and double glazed windows, respectively.

(2) Lower solar transmittance in clear state and higher solar transmittance modulation ability exhibit a positive effect on the building energy performance in hot climates.

(3) TC glazing with higher luminous transmittance and relatively lower luminous transmittance modulation ability was desirable to reduce building energy use and enhance indoor daylight availability.

(4) The Pareto frontier solutions for the single and double glazed windows have been obtained. And the trade-off optimization shows that the lowest building energy consumption was accompanied by the worst daylight performance in the Pareto frontier.

(5) The Pareto-optimal solution (POS) has been obtained from the Pareto frontier set. The selected hypothetical TC windows can improve the building energy and daylighting performance simultaneously when compared with traditional clear single and double glazed windows. The POS can provide technical guidance for the practical development of TC materials.

Table 6 Bi-objective optimization results of the TC coating for single and double glazed windows

	TC for single glazed windows			TC for double glazed windows		
Design parameters	A/E_{min}	B/ $UDI_{300-3000\ max}$	C/POS	A/E_{min}	B/ $UDI_{300-3000\ max}$	C/POS
τ_t	34.8	28.7	29.8	33.3	29.2	29.8
T_{solar}	0.38	0.38	0.38	0.45	0.45	0.45
ΔT_{solar}	0.26	0.18	0.21	0.27	0.19	0.26
T_{lum}	0.76	0.76	0.76	0.9	0.89	0.89
ΔT_{lum}	0.52	0.47	0.41	0.55	0.54	0.51

(6) Compared with the single-objective optimizations, the Pareto optimization is more suitable for decision-makers finding the desired solution based on their preferences and engineering experiences.

Acknowledgements

This work was supported by the National Natural Science Foundation of China (No. 51878581 and No. 51778549) and the Fundamental Research Funds for the Central Universities (No. 20720200087).

References

Abdollahzadeh N, Tahsildoost M, Zomorodian ZS (2020). A method of partition design for open-plan offices based on daylight performance evaluation. *Journal of Building Engineering*, 29: 101171.

Aburas M, Soebarto V, Williamson T, et al. (2019). Thermochromic smart window technologies for building application: A review. *Applied Energy*, 255: 113522.

Ataalla M, Afify AS, Hassan M, et al. (2018). Tungsten-based glasses for photochromic, electrochromic, gas sensors, and related applications: A review. *Journal of Non-Crystalline Solids*, 491: 43–54.

Bader J, Deb K, Zitzler E (2010). Faster hypervolume-based search using Monte Carlo sampling. In: Ehrgott M, Naujoks B, Stewart T, et al. (eds), Multiple Criteria Decision Making for Sustainable Energy and Transportation Systems. Lecture Notes in Economics and Mathematical Systems, vol 634. Berlin: Springer.

Bader J, Zitzler E (2011). HypE: An algorithm for fast hypervolume-based many-objective optimization. *Evolutionary Computation*, 19: 45–76.

Baetens RB, Jelle BP, Gustavsen A (2010). Properties, requirements and possibilities of smart windows for dynamic daylight and solar energy control in buildings: A state-of-the-art review. *Solar Energy Materials and Solar Cells*, 94: 87–105.

Blackman CS, Piccirillo C, Binions R, et al. (2009). Atmospheric pressure chemical vapour deposition of thermochromic tungsten doped vanadium dioxide thin films for use in architectural glazing. *Thin Solid Films*, 517: 4565–4570.

BSI (2011). BS EN 12464-1. 2011 Light and Lighting—Lighting of Work Places—Part 1: Indoor Work Places, BSI Standard.

Cao X, Chang T, Shao Z, et al. (2020). Challenges and opportunities toward real application of VO²-based smart glazing. *Matter*, 2: 862–881.

Chen D, Zhang Y, Bessho T, et al. (2015). Formation of reflective and conductive silver film on ABS surface via covalent grafting and solution spray. *Applied Surface Science*, 349: 503–509.

Cui Y, Ke Y, Liu C, et al. (2018). Thermochromic VO_2 for energy-efficient smart windows. *Joule*, 2: 1707–1746.

DOE (2016). EnergyplusTM Version 8.5 Documentation: Engineering Reference. US Department of Energy.

Eltaweel A, Su Y (2017). Controlling venetian blinds based on parametric design; via implementing Grasshopper's plugins: A case study of an office building in Cairo. *Energy and Buildings*, 139: 31–43.

EnergyPlus (2020). Weather Data from EnergyPlus. Available at: https://energyplus.net/weather-region/asia_wmo_region_2/CHN%20%20. Accessed 15 Sept 2020.

Fabiani C, Pisello AL, Bou-Zeid E, et al. (2019). Adaptive measures for mitigating urban heat islands: The potential of thermochromic materials to control roofing energy balance. *Applied Energy*, 247: 155–170.

Fabiani C, Castaldo VL, Pisello Al (2020). Thermochromic materials for indoor thermal comfort improvement: Finite difference modeling and validation in a real case-study building. *Applied Energy*, 262: 114147.

Feng W, Zou L, Gao G, et al. (2016). Gasochromic smart window: optical and thermal properties, energy simulation and feasibility analysis. *Solar Energy Materials and Solar Cells*, 144: 316–323.

Garcia G, Buonsanti R, Llordes A, et al. (2013). Near-infrared spectrally selective plasmonic electrochromic thin films. *Advanced Optical Materials*, 1: 215–220.

Giovannini L, Favoino F, Pellegrino A, et al. (2019). Thermochromic glazing performance: From component experimental characterisation to whole building performance evaluation. *Applied Energy*, 251: 113335.

Guo C, Yin S, Yan M, et al. (2011). Facile synthesis of homogeneous CsxWO3 nanorods with excellent low-emissivity and NIR shielding property by a water controlled-release process. *Journal of Materials Chemistry*, 21: 5099–5105.

Hoffmann S, Lee ES, Clavero C (2014). Examination of the technical potential of near-infrared switching thermochromic windows for commercial building applications. *Solar Energy Materials and Solar Cells*, 123: 65–80.

Hosseini SM, Mohammadi M, Guerra-Santin O (2019). Interactive kinetic façade: Improving visual comfort based on dynamic daylight and occupant's positions by 2D and 3D shape changes. *Building and Environment*, 165: 106396.

Hu JY, Yu X (2019a). Design and characterization of energy efficient roofing system with innovative TiO2 enhanced thermochromic films. *Construction and Building Materials*, 223: 1053–1062.

Hu JY, Yu X (2019b). Adaptive thermochromic roof system: Assessment of performance under different climates. *Energy and Buildings*, 192: 1–14.

Huang Z, Chen C, Lv C, et al. (2013). Tungsten-doped vanadium dioxide thin films on borosilicate glass for smart window application. *Journal of Alloys and Compounds*, 564: 158–161.

JGJ/T449 (2018). Standard for Green Performance Calculation of Civil Building. (in Chinese).

Lee ES, Fernandes LL, Goudey CH, et al. (2013a). A pilot demonstration of electrochromic and thermochromic windows in the denver federal center, building 41, Denver, CO, USA.

Lee ES, Pang XF, Hoffmann S, et al. (2013b). An empirical study of a full-scale polymer thermochromic window and its implications on material science development objectives. *Solar Energy Materials and Solar Cells*, 116: 14–26.

Li S, Niklasson GA, Granqvist CG (2014). Thermochromic undoped and Mg-doped VO_2 thin films and nanoparticles: Optical properties and performance limits for energy efficient windows. *Journal of Applied Physics*, 115: 053513.

Liang R, Sun Y, Aburas M, et al. (2018). Evaluation of the thermal and optical performance of thermochromic windows for office buildings in China. *Energy and Buildings*, 176: 216–231.

Liang R, Sun Y, Aburas M, et al. (2019). An exploration of the combined effects of NIR and VIS spectrally selective thermochromic materials on building performance. *Energy and Buildings*, 201: 149–162.

Long L, Ye H (2014). Discussion of the performance improvement of thermochromic smart glazing applied in passive buildings. *Solar Energy*, 107: 236–244.

Long L, Ye H, Gao Y, et al. (2014). Performance demonstration and evaluation of the synergetic application of vanadium dioxide glazing and phase change material in passive buildings. *Applied Energy*, 136: 89–97.

Long L, Ye H, Zhang H, et al. (2015). Performance demonstration and simulation of thermochromic double glazing in building applications. *Solar Energy*, 120: 55–64.

Long L, Ye H (2016). Nano-based chromogenic technologies for building energy efficiency. In: Pacheco-Torgal F, Rasmussen E, Granqvist C-G, et al. (eds), Start-Up Creation. Cambridge, UK: Woodhead Publishing.

Long L, Ye H (2017). Dual-intelligent windows regulating both solar and long-wave radiations dynamically. *Solar Energy Materials and Solar Cells*, 169: 145–150.

Mahmoud AHA, Elghazi Y (2016). Parametric-based designs for kinetic facades to optimize daylight performance: Comparing rotation and translation kinetic motion for hexagonal facade patterns. *Solar Energy*, 126: 111–127.

Mostapha SR, Sarith S (2016). Automating radiance workflows with Python. In: Proceedings of the 15th Annual Radiance Workshop, Padua, Italy.

Pilechiha P, Mahdavinejad M, Pour Rahimian F, et al. (2020). Multi-objective optimisation framework for designing office windows: Quality of view, daylight and energy efficiency. *Applied Energy*, 261: 114356.

Saeli M, Piccirillo C, Parkin IP, et al. (2010a). Energy modelling studies of thermochromic glazing. *Energy and Buildings*, 42: 1666–1673.

Saeli M, Piccirillo C, Parkin IP, et al. (2010b). Nano-composite thermochromic thin films and their application in energy-efficient glazing. *Solar Energy Materials and Solar Cells*, 94: 141–151.

Soumya S, Mohamed AP, Mohan K, et al. (2015). Enhanced near-infrared reflectance and functional characteristics of Al-doped ZnO nano-pigments embedded PMMA coatings. *Solar Energy Materials and Solar Cells*, 143: 335–346.

Sun Y, Wilson R, Wu Y (2018). A Review of Transparent Insulation Material (TIM) for building energy saving and daylight comfort. *Applied Energy*, 226: 713–729.

Tällberg R, Jelle BP, Loonen R, et al. (2019). Comparison of the energy saving potential of adaptive and controllable smart windows: A state-of-the-art review and simulation studies of thermochromic, photochromic and electrochromic technologies. *Solar Energy Materials and Solar Cells*, 200: 109828.

Warwick MEA, Ridley I, Binions R (2014). The effect of transition gradient in thermochromic glazing systems. *Energy and Buildings* 77: 80–90.

Xu X, Wu Xi, Zhao C, et al. (2012). Simulation and improvement of energy consumption on intelligent glasses in typical cities of China. *Science China Technological Sciences*, 55: 1999–2005.

Yang Y-S, Zhou Y, Chiang FBY, et al. (2017). Tungsten doped VO_2/microgels hybrid thermochromic material and its smart window application. *RSC Advances*, 7: 7758–7762.

Ye H, Long L, Zhang H, et al. (2013). The demonstration and simulation of the application performance of the vanadium dioxide single glazing. *Solar Energy Materials and Solar Cells*, 117: 168–173.

Ye H, Long L (2014). Smart or not? A theoretical discussion on the smart regulation capacity of vanadium dioxide glazing. *Solar Energy Materials and Solar Cells*, 120: 669–674.

Ye H, Long L, Zhang H, et al. (2014). The energy saving index and the performance evaluation of thermochromic windows in passive buildings. *Renewable Energy*, 66: 215–221.

Zhang Y, Tso CY, Inigo JS, et al. (2019). Perovskite thermochromic smart window: Advanced optical properties and low transition temperature. *Applied Energy*, 254: 113690.

Zhang Y, Zhai X (2019). Preparation and testing of thermochromic coatings for buildings. *Solar Energy*, 191: 540–548.

Zhang Y, Zhu Y, Yang J, et al. (2020). Energy saving performance of thermochromic coatings with different colors for buildings. *Energy and Buildings*, 215: 109920.

Zheng L, Xiong T, Shah KW (2019). Transparent nanomaterial-based solar cool coatings: Synthesis, morphologies and applications. *Solar Energy*, 193: 837–858.